JOURNAL OF MATERIALS SCIENCE 25 (1990) 5118–5124

Oxidation of SiC–ZrO_2 composites

W. LUECKE, D. L. KOHLSTEDT*
Department of Materials Science and Engineering, Cornell University, Ithaca, New York 14853-1501, USA

S. B. DAWES
Corning Glass Works, Sullivan Park Research Center, Corning, New York 14830, USA

Planar silicon carbide–zirconium oxide composites were oxidized at temperatures between 910 and 1050° C in oxygen, argon and CO–CO_2 atmospheres. In addition, bare SiC substrates were oxidized in oxygen. The bare substrates showed parabolic oxidation kinetics. The oxidation kinetics of the composites were more difficult to interpret because of the solid state reaction between the ZrO_2 and the SiO_2, but were approximately parabolic.

1. Introduction

In the production of SiC–glass composites, a barrier layer is often placed between the SiC fibre and the glass matrix to prevent the interaction of the cations in the glass with the SiC. In addition, this layer is often needed to modify the adhesion between the glass and the fibre, increasing the fracture toughness by optimizing the bonding between fibre and matrix. The barrier layer can interact chemically with the fibre, as well, either during processing or service of the composite. If this interaction can be controlled and understood, the mechanical properties of the resulting composite can be more precisely controlled.

The oxidation kinetics of SiC–ZrO_2 composites have been studied as well as those of bare SiC substrates to understand better the interaction of a barrier layer with SiC in a model system. ZrO_2 was chosen because it is simpler than many of the other barrier layers, and because low cation diffusivities in ZrO_2 should make it an excellent cation barrier. Rather than working with fibres, a two-dimensional composite was chosen: a flat substrate of SiC coated with a thin layer of ZrO_2. This sample geometry simplifies the calculation of the oxidation kinetics, and enables Rutherford backscattering spectrometry (RBS) to be used to measure the oxide layer thickness. The oxidation kinetics of this model system were measured as a function of temperature, ZrO_2 layer thickness, and oxygen partial pressure. In addition, the solid state reaction between the ZrO_2 and the SiO_2 which forms during oxidation was observed.

2. Experimental procedure

The composites used in these experiments were substrates of Ceradyne (Ceralloy 146IG α-SiC: Ceradyne Inc., Santa Ana, California) α-phase SiC covered by a thin layer of ZrO_2. Table I shows the major impurities in the hot-pressed Ceradyne SiC, as determined by optical emission spectroscopy (3.4 m Ebert optical emission spectrograph). A zirconia precursor sol was produced by refluxing 0.0099 kg of $Zr(OC_4H_9)_4 \cdot C_4H_9$ in a solution of 85 ml 2-methoxy ethanol plus 3 ml HNO_3. This sol was spun on to the polished surface of the substrate using a photoresist spinner for 1 min at 2000 r.p.m. The zirconia gel coating that resulted was converted to ZrO_2 by firing to 600° C in air at 20° C min^{-1} and then to 900° C in forming gas. This firing schedule produced a ZrO_2 layer about 10 nm thick. Repeating this process produced thicker layers.

The two-layer composites were oxidized in an alumina tube furnace under either oxygen, argon or mixtures of CO–CO_2 gas. The gases were not dried before use, and were of commercial purity. While in the furnace, the samples hung from the end of a type R thermocouple (Pt/Pt–13% Rh) in either an alumina or zirconia crucible. The oxygen partial pressure in the furnace tube was monitored using a zirconia oxygen sensor. The specimens were oxidized for a given time and then quenched to room temperature still under gas. After analyses to determine the thickness of the SiO_2 layer and the composition of the surface layers, the specimens were returned to the furnace for further oxidation.

The thickness of the SiO_2 layer that formed during oxidation was determined by analysing Rutherford backscattering spectra of the specimens. A backscattering spectrum from the sample, using 2.8 MeV α-particles as the probe beam, was collected after each oxidation. The α-particle beam sampled an area of the specimen approximately 1 mm^2. To convert the areal density of the SiO_2 layer which was calculated from the backscattering spectrum to thickness, the density of SiO_2 was assumed to be 2.3×10^{23} mol cm^{-3}. In many cases, an X-ray diffraction pattern (Scintag PAD X diffractometer, Scintag, Santa Clara, California) using Cu$K\alpha$ radiation (λ = 0.154 059 nm), was also collected so that the phases present in the near surface layers (ZrO_2, $ZrSiO_4$, and SiO_2) could be identified.

3. Results and discussion

The oxidation kinetics of these ZrO_2–SiC composites

Present address Department of Geology and Geophysics, University of Minnesota, Minneapolis, MN, 55455, USA.

0022–2461/90 $03.00 + .12

TABLE I Trace impurities in the Ceradyne α-SiC as determined by atomic absorbtion analysis

Impurity	wt %
B	0.3–1.0
Al, Fe	0.03–0.1
Ca	0.01–0.03
Cr, Mn, Ti, V	Trace

were determined as a function of temperature (910° C < T < 1069° C) in pure oxygen. At two temperatures (970 and 1069° C), the oxidation kinetics were investigated as a function of ZrO_2 thickness, and at a lower temperature (910° C), the oxidation kinetics were measured as a function of oxygen partial pressure. It was observed that at higher oxidation temperatures the SiO_2 which forms reacts with the ZrO_2 to form $ZrSiO_4$. Finally, we oxidized a set of bare substrates so that we may more accurately assess the effect of the ZrO_2 surface layer on the oxidation kinetics. The bare substrate oxidation kinetics will be discussed first.

3.1. Substrate oxidation kinetics

The thickness of the SiO_2 layer which grows on the SiC substrate during oxidation was measured by analysing Rutherford backscattering spectra from the oxidized specimens. In RBS, a monoenergetic beam of α-particles (here 2.8 MeV) is incident upon the sample. A silicon barrier detector coupled to a multichannel analyzer identifies the number and energy of α-particles scattered through large angles by nuclei in the target. The spectrum collected is plotted as the yield of α-particles as a function of their energy. There is not space here to discuss in great detail the interpretation of backscattering spectra; the interested reader is referred to an excellent publication [1]. Briefly, though, there are three fundamentals to interpreting an RBS spectrum.

1. The energy of an α-particle scattered from a target nucleus on the surface of the specimen, for fixed detector position, is a function only of the incident energy of the particle and the atomic number of the target nucleus. The α-particles scattered from heavy nuclei return with a greater fraction of their incident energy than those scattered from lighter nuclei. A homogeneous, multi-element target produces a spectrum which resembles a set of stairs, each stair step arising from the contribution of another element. The energies at which sharp changes in yield occur can be used to identify the elements in a target of unknown composition.

2. The probability that a target nucleus will scatter an incident α-particle is roughly proportional to both the square of the atomic number of the target atoms as well as to the areal density of target atoms, measured in units of atoms cm^{-2}. Because zirconium is so much heavier than carbon, just a little zirconium produces a large signal in the spectrum. In addition, the yield from silicon in SiO_2 will be less than that from silicon in SiC because there are fewer silicon atoms in the path of the beam in SiO_2. By analysing the shape of the spectrum a compositional analysis of the target can be made.

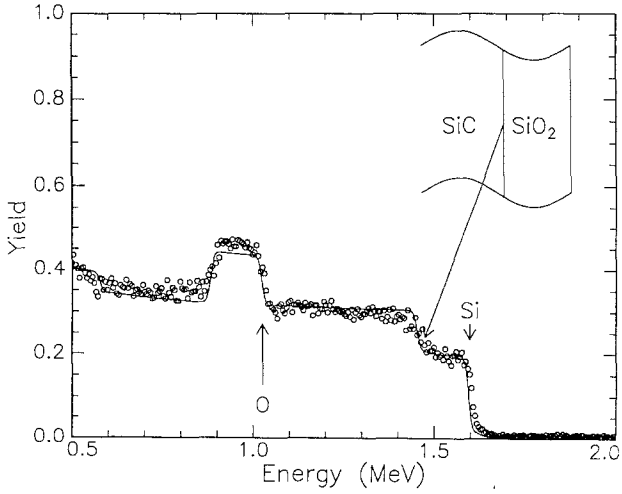

Figure 1 Backscattering spectrum from an SiC substrate oxidized for 21.4 h at 970° C in oxygen. (——) simulation, $\Delta\xi = 0.24\,\mu m$.

3. The α-particles which penetrate into the target before being scattered lose energy to interactions with the k-shell electrons of the target. Typically, this energy loss amounts to 100 to 1000 eV nm^{-1}, thus limiting the volume probed to the top several micrometres of the specimen. An α-particle scattered by a nucleus deep in the target will return to the detector with less energy than one scattered from a target nucleus at the surface. Because the energy loss can be calculated for any target, we can calculate a composition profile for the target from its spectrum.

Fig. 1 is a backscattering spectrum from an SiC substrate oxidized in oxygen for 21.4 h at 970° C. The step in the yield at 1.6 MeV originates from scattering by silicon nuclei in the SiO_2 at the surface. Correspondingly, the step in yield at 1.0 MeV comes from scattering by oxygen nuclei in the SiO_2 layer. The third step in the yield, at 1.4 MeV, comes about because the areal density of silicon in the SiC of the composite is greater than that in SiO_2. This edge marks the boundary between the SiO_2 and the SiC substrate. The spectrum provides two independent measures of the SiO_2 layer-thickness: (1) the width of the step in the silicon signal and (2) the width of the hump from the oxygen in the SiO_2 layer. Lying over the data points is a simulation of the spectrum calculated with the modelling program described by Doolittle [2]. The modelling program takes as input a description of the sample as a stack of constant composition slabs, such as that shown in the upper right-hand corner of Fig. 1, as well as the spectrum acquisition parameters. The only free parameter in the simulation is the thickness of the SiO_2 layer, which is varied until the χ^2 error between the simulation and the actual spectrum is a minimum. In this spectrum the SiO_2 layer is 0.24 μm thick.

Several subtle features of the spectrum are worth noting. The scattering cross-sections for boron and carbon are so low that these elements are essentially invisible. Carbon in the SiC should produce a step in yield at 0.6 MeV; the noise in the spectrum totally obscures that increase. The simulation also predicts that the yield–energy curve should be steeper than it actually is both at 1.4 and 0.85 MeV. This shallowness

of the spectrum indicates that the interface between the SiO_2 and the SiC is not planar, as depicted in Fig. 1. A planar SiC–SiO_2 interface implies a discontinuity in the areal density of silicon, which gives rise to a vertical step in the yield in the backscattering spectrum. Because the interface is characterized by a non-vertical step in the yield from silicon, the areal density of silicon must be varying continuously in the region of the interface. A rough interface means that some SiC, with its greater areal density of silicon, projects above the average position of the interface, making the yield from silicon higher than the simulation predicts. Similarly, SiO_2, with its smaller areal density of silicon, projects below the average position of the interface, making the yield from silicon lower than the simulation predicts. That the interface is non-uniform is not surprising, because the oxidation rate of SiC is highly orientation dependent [3], varying by a factor of up to seven [4] from one orientation to the next. The individual, randomly oriented, grains in the substrate oxidize at different rates, producing a rough interface.

The square of the oxide layer thickness is plotted as a function of time for three temperatures in Fig. 2. The best-fit lines are the linear least squares fit to the data, not constrained to pass through zero. The oxidation kinetics are parabolic in time, suggesting that mass transport through the SiO_2 layer, rather than the oxidation reaction to form SiO_2, limits the rate of oxidation. Whether the species whose diffusion limits the rate of reaction is molecular or atomic oxygen cannot be determined.

Each of the curves in Fig. 2 yields a parabolic reaction rate constant, k_p, of the form

$$\Delta\xi^2 = 2k_p t \quad (1)$$

where $\Delta\xi$ is the thickness of the SiO_2 layer and t is the oxidation time. The parabolic reaction rate constants determined from the slopes of the best fit lines are displayed in Fig. 2. These parabolic reaction rate constants are also plotted on an Arrhenius plot in Fig. 3. The uncertainty associated with each data point is of the order of the symbol size. The activation energy for oxidation is $209 \pm 9\,kJ\,mol^{-1}$. Also plotted in Fig. 3

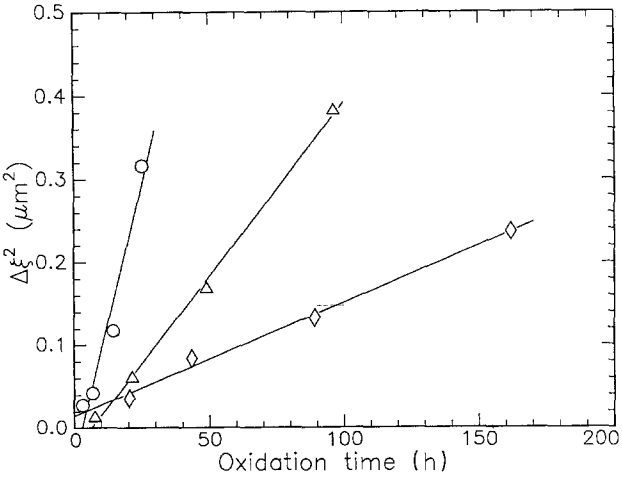

Figure 2 Square of the oxide layer thickness as a function of oxidation time for bare substrates oxidized in oxygen. (○) 1050° C, $k_p = 6.6 \times 10^{-3}\,\mu m^2 h^{-1}$; (△) 970° C, $k_p = 2.1 \times 10^{-3}\,\mu m^2 h^{-1}$; (◇) 910° C, $k_p = 6.9 \times 10^{-4}\,\mu m^2 h^{-1}$.

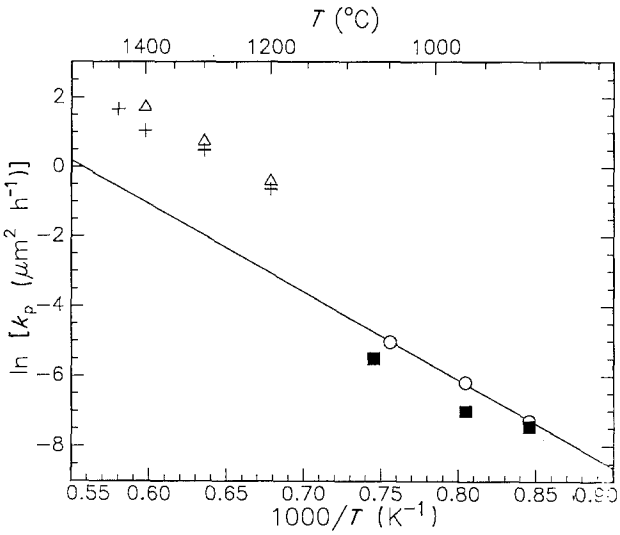

Figure 3 Logarithm of the parabolic reaction rate constant, k_p, as a function of inverse temperature. (○) SiC substrates; (△) [3], hot pressed; (+) [3], sintered; (■) 55 nm ZrO_2. $Q = 209 \pm 9\,kJ\,mol^{-1}$.

are data from Costello and Tressler [3] for the oxidation of both hot-pressed and sintered α-SiC. The sintered α-SiC studied there has approximately the same impurity content as the SiC studied here. The oxidation rate measured here is approximately ten times slower than that given by Costello and Tressler [3], when extrapolated to their higher oxidation temperatures. Their activation energies, about $220\,kJ\,mol^{-1}$, are comparable to ours. The reason for the discrepancy in the absolute magnitude of the parabolic reaction rate constants between those measured here and the extrapolation of those described by Costello and Tressler [3] is not clear. Given that trace amounts of water vapour increase the oxidation rate of SiC [5, 6], it is especially interesting that the oxidation rate measured here is slower than that measured by Costello and Tressler [3] in which oxidation was done in dry oxygen.

3.2. Oxidation of the composites

3.2.1. Microstructural observations

Qualitatively, the backscattering spectra from the ZrO_2-coated SiC substrates resemble those from the uncoated substrates. Fig. 4 shows the spectrum from

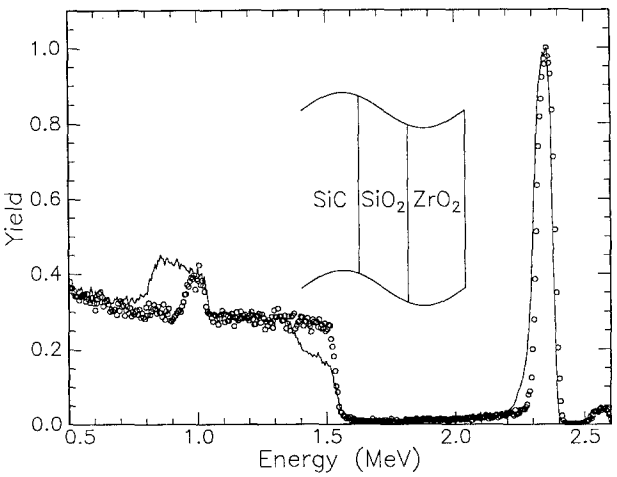

Figure 4 Backscattering spectrum from a ZrO_2–SiC composite oxidized for 47.7 h at 970° C. (○) Unoxidized, (——) 970° C, 47.7 h.

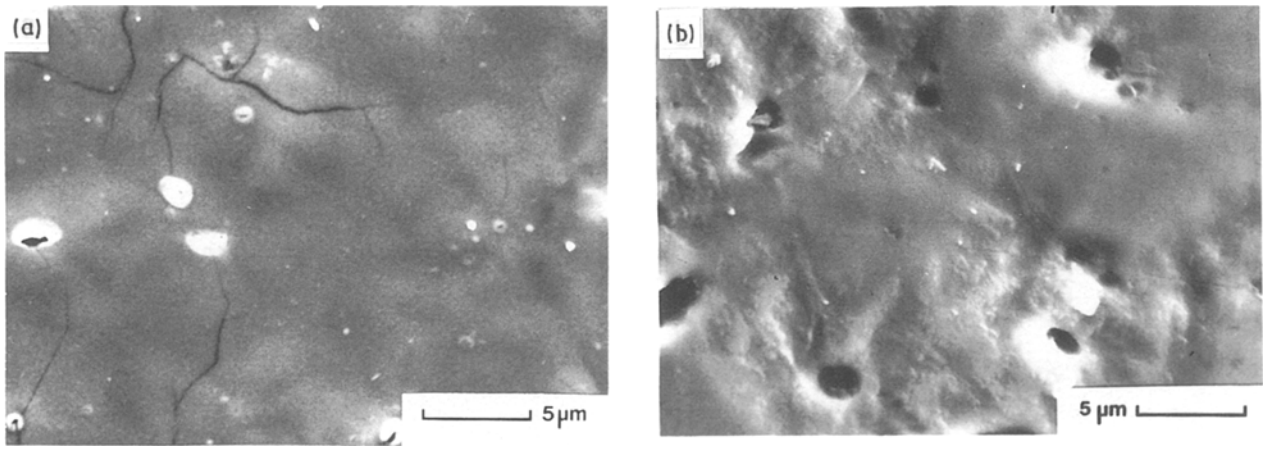

Figure 5 (a) Scanning electron micrograph of the surface of an SiC–ZrO_2 composite oxidized 145 h at 970° C in oxygen. The oxide layer is greater than 0.8 μm thick. (b) The surface of the same specimen after all the SiO_2 was removed by etching in hydrofluoric acid.

an unoxidized composite with a 70 nm thick ZrO_2 layer. Superimposed upon this spectrum is the spectrum from the same sample oxidized for 47.7 h at 970° C in oxygen. The most notable difference in the spectra from the ZrO_2 coated specimens with respect to those from the uncoated specimens is the appearance at 2.4 MeV of a large peak from the zirconium in the surface layer. The small peak at 1.0 MeV comes from the oxygen in the ZrO_2 in the surface layer as well as that in a thin layer of SiO_2 which forms during the transformation of the zirconium sol to ZrO_2. The tiny peak just visible at 2.5 MeV is due to a 0.01 at % hafnium impurity in the precursor sol. The growth of the SiO_2 layer manifests itself in the same way as in the spectra from the uncoated specimens. A shelf appears in the edge of the silicon signal, while the oxygen peak at 1.0 MeV widens. The specimen is modelled as shown by the schematic cross-section in the upper right-hand corner of Fig. 4. The thickness of the ZrO_2 layer was calculated from the spectrum from the unoxidized material. As with the uncoated specimens, the SiO_2 layer thickness was calculated by finding the thickness which minimized the χ^2 error between the simulated and actual spectra. For the spectrum shown in Fig. 4 the SiO_2 layer is 0.26 μm thick.

The slope of the yield–energy curve in the region of the SiO_2–SiC interface shows that the SiO_2 layer is not of uniform thickness. Scanning electron micrographs, such as that shown in Fig. 5a, demonstrate that the surface of the oxidized composite remains flat even after the oxide layer grows as thick as 0.8 μm. The small cracks visible on the surface of the specimen in the micrograph probably formed during the repeated quenching and reheating of the sample due to the mismatch in the thermal expansion coefficients between the substate and the oxide layer. Clearly, these cracks will be short circuit transport paths for oxygen, and are probably partly responsible for the deviation from parabolic oxidation kinetics at long oxidation times. When the layer of SiO_2 is stripped off the sample by etching in hydrofluoric acid, the SiC surface remaining shows the texture of the original SiO_2–SiC interface. Fig. 5b is a scanning electron micrograph of the surface of the sample shown in Fig. 5a, after all the SiO_2 and ZrO_2 have been stripped off. Clearly, most of the roughness is at the SiO_2–SiC interface rather than the surface of the sample.

At the highest oxidation temperature (1069° C) the ZrO_2 surface coating quickly reacts with the SiO_2 layer to form zircon, $ZrSiO_4$. At this temperature, the thinnest ZrO_2 coatings (27 nm) had completely reacted to form zircon after only 3.35 h, while the thickest coatings (70 nm) required over 100 h to completely transform. At 970° C some zircon formed as the oxidation progressed, but after 145 h oxidation the surface layer remained predominantly ZrO_2 for all thicknesses of ZrO_2. No zircon formed when the ZrO_2–SiC composites were oxidized at 910° C, even after 162 h.

Evidence of zircon formation is present in both the X-ray diffractometer traces and the backscattering spectra. After oxidation an X-ray diffractometer trace was acquired from each specimen. Rather than relying upon the literature values for the SiC and ZrO_2 peak positions, we also made X-ray diffractometer traces from the bare substrate and from ZrO_2 powder made from the sol and heat treated identically to the composites. No such standard was used for zircon. Fig. 6 is such a trace from a composite oxidized in oxygen for 24.8 h at 1069° C. The three strong peaks in the range 0.249 nm $< d <$ 0.264 nm come from the SiC

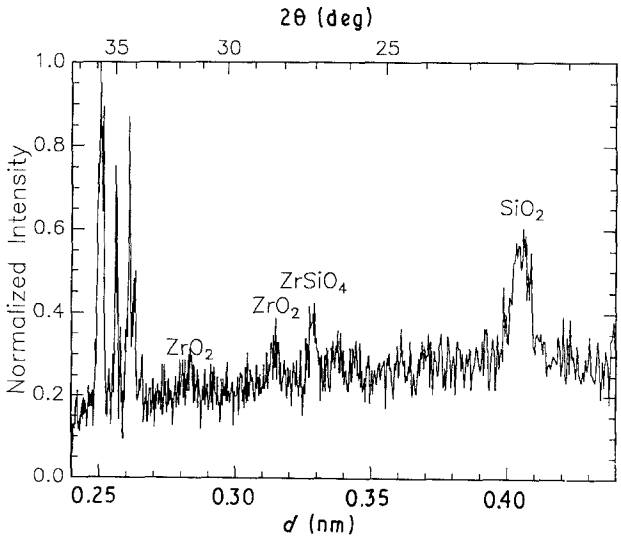

Figure 6 X-ray diffractometer trace from a ZrO_2–SiC composite oxidized 45.1 h at 1069° C in oxygen.

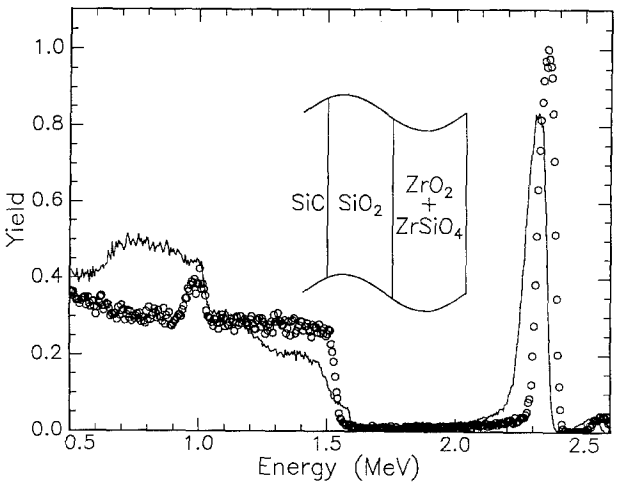

Figure 7 RBS spectra from (○) an unoxidized ZrO_2–SiC composite and (——) the same specimen oxidized in oxygen for 45.1 h at 1069° C.

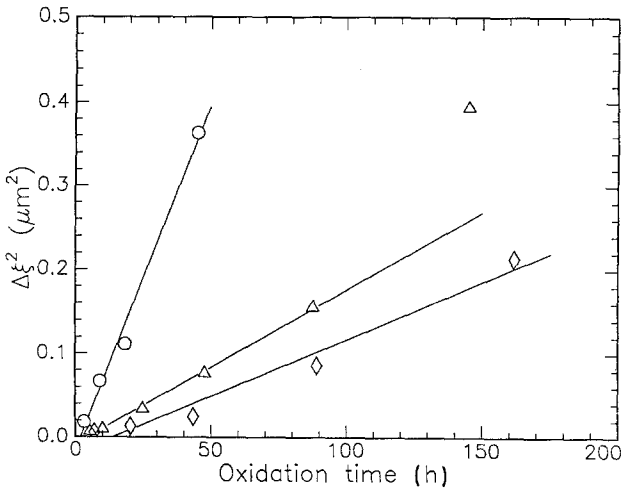

Figure 8 Square of the SiO_2 layer thickness as a function of oxidation time at three temperatures for composites with 55 nm ZrO_2 coating. (○) 1069° C, $k_p = 4.1 \times 10^{-3}\,\mu m^2 h^{-1}$; (△) 970° C, $k_p = 9.2 \times 10^{-4}\,\mu m^2 h^{-1}$; (◇) 910° C, $k_p = 6.9 \times 10^{-4}\,\mu m^2 h^{-1}$.

substrate. The two very weak peaks at $d = 0.3178$ and 0.2847 nm are from the ZrO_2 in the surface layer, while the larger peak at $d = 0.3276$ nm comes from the $ZrSiO_4$ in the surface layer. The very large peak at $d = 0.4051$ nm is from crystalline SiO_2, as cristobalite, in the oxidized layer.

There is evidence for the ZrO_2 to $ZrSiO_4$ transformation in the backscattering spectrum from this sample as well. Fig. 7 shows two spectra, one from a composite before oxidation and the second from the same specimen after oxidation. The SiO_2 layer which has grown between the SiC and the ZrO_2 layer is 0.44 μm thick. There are two pieces of evidence pointing towards the formation of $ZrSiO_4$. The zirconium peak height has dropped to 81% of its initial value and has broadened, but the integral under the zirconium peak has remained constant. Therefore, the amount of zirconium cannot have changed during the heat treatment, but its areal density must have decreased, consistent with the addition of SiO_2 to the layer. The second piece of evidence is the appearance of a second shelf in the spectrum just above 1.5 MeV. The signal from silicon now appears at a greater energy than it does in the unoxidized specimen. The energy at which the small shelf appears indicates that there is silicon at the surface of the specimen, as there should be if the surface layer is $ZrSiO_4$. The small shift in the zirconium peak position between the two spectra occurred because they were acquired at slightly different beam energies. It is important to note that the X-ray diffractometer trace is necessary to identify completely the new phase as zircon. RBS is incapable of discriminating a 1 : 1 mixture of SiO_2 and ZrO_2 from $ZrSiO_4$.

3.2.2. Oxidation kinetics

The oxidation kinetics of the ZrO_2–SiC composites are comparable in magnitude to those of the uncoated substrates, though slightly slower. Though the substrates oxidize more slowly, the growth of the oxide layer still follows a parabolic law. Fig. 8 shows the square of the oxide layer thickness as a function of time for several temperatures for composites having a 55 nm thick ZrO_2 layer. The 150 h datum for the specimen oxidized at 970° C has not been included in the calculation of the best fit line because the surface of the specimen was extensively cracked. This sample had been quenched to room temperature six times during the 150 h oxidation. The parabolic reaction rate constants for this set of specimens are also plotted on the Arrhenius plot in Fig. 3. At higher temperatures, the ZrO_2–SiC composites oxidize slightly more slowly than the uncoated substrates, though at 910° C the rates of oxidation are nearly equal. Because at temperatures greater than 910° C the ZrO_2 and the SiO_2 react to form zircon, thus changing the nature of the surface layer, an activation energy calculation for the oxidation has little meaning. The parabolic reaction rate constants are only overlayed in Fig. 3 for ease of comparison with the constants from the bare substrate oxidation.

Thicker ZrO_2 layers improve the oxidation resistance of the SiC substrate, though not dramatically. Fig. 9 shows the square of the oxide layer thickness as a function of time for three thicknesses of ZrO_2 as well as that for the uncoated substrate, all oxidized in

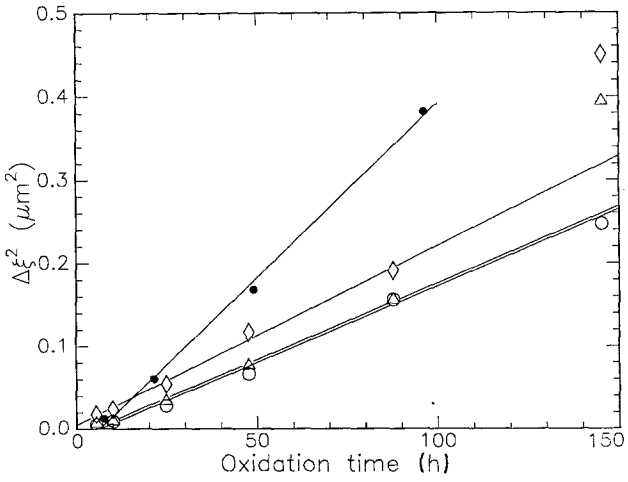

Figure 9 Square of the SiO_2 thickness as a function of oxidation time for three thicknesses of ZrO_2 as well as the uncoated substrate for composites oxidized in oxygen at 970° C. (○) 70 nm ZrO_2, $k_p = 9.0 \times 10^{-4}\,\mu m^2 h^{-1}$; (△) 55 nm ZrO_2, $k_p = 9.2 \times 10^{-4}\,\mu m^2 h^{-1}$; (◇) 27 nm ZrO_2. $k_p = 1.1 \times 10^{-3}\,\mu m^2 h^{-1}$; (●) bare substrate, $k_p = 2.1 \times 10^{-3}\,\mu m^2 h^{-1}$.

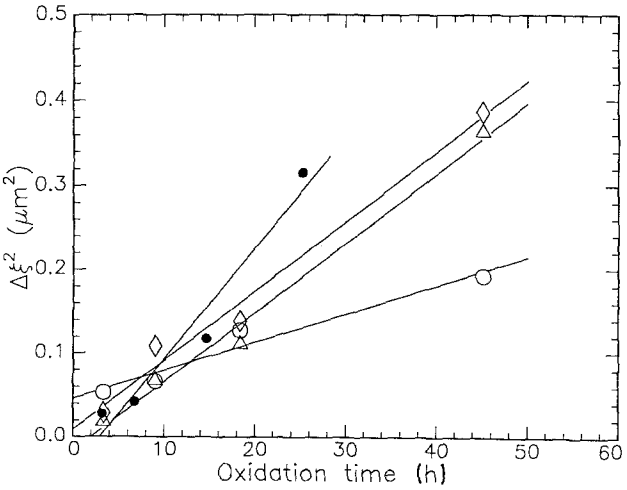

Figure 10 Square of the SiO_2 thickness as a function of oxidation time for three thicknesses of ZrO_2 as well as the uncoated substrate for composites oxidized in oxygen at 1069° C. (○) 70 nm ZrO_2, $k_p = 1.7 \times 10^{-3} \mu m^2 h^{-1}$; (△) 55 nm ZrO_2, $k_p = 4.1 \times 10^{-3} \mu m^2 h^{-1}$; (◇) 27 nm ZrO_2, $k_p = 4.2 \times 10^{-3} \mu m^2 h^{-1}$; (●) bare substrate, $k_p = 6.6 \times 10^{-3} \mu m^2 h^{-1}$.

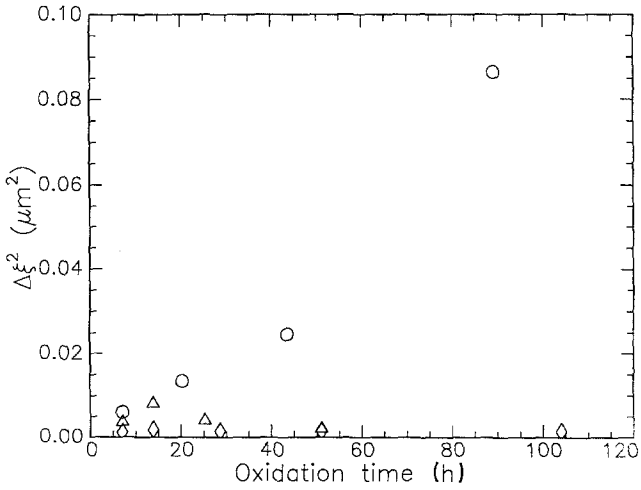

Figure 11 Square of the oxide layer thickness as a function of time for composites oxidized at 910° C in different oxygen partial pressures. (○) $\log_{10} p_{O_2} = 0$ (oxygen), (△) $\log_{10} p_{O_2} = -2.8$ (argon), (◇) $\log_{10} p_{O_2} = -13.4$ (CO–CO_2).

oxygen at 970° C. The composite with the thinnest coating shows the greatest oxidation rate, while the two more thickly coated composites showed nearly identical, slower oxidation rates. The parabolic reaction rate constants are summarized in the caption of Fig. 9. The best fit lines for the data from the two samples with thinner coatings are not constrained to pass through the points at 150 h.

Similar oxidation behaviour occurs at 1069° C, as well. Fig. 10 shows the square of the oxide layer thickness for the same three thicknesses of ZrO_2 as shown in Fig. 9, along with that for the bare substrate. Generally, the specimens showed parabolic oxidation kinetics. The two specimens with the thinner coatings showed unusual oxidation behaviour. The oxide layer thickness follows a $t^{1/2}$ dependence, but the best fit line does not extrapolate back to near zero thickness at the start of the oxidation.

When the composites were oxidized at low oxygen partial pressures, the thin oxide layer formed during the conversion of the precursor to ZrO_2 did not grow thicker. Fig. 11 compares the square of the oxide layer thickness as a function of time for composites oxidized at 910° C in oxygen ($p_{O_2} = 10^5$ Pa), argon ($p_{O_2} = 10^{3.8}$ Pa), and a CO–CO_2 mixture ($p_{O_2} = 10^{-8.4}$ Pa). That the SiO_2 layer did not grow is not surprising. The parabolic reaction rate constant for oxidation of SiO_2 is proportional to the square root of the oxygen partial pressure at temperatures above 1300° C [7, 8]. If the same dependence holds at 910° C, the predicted oxidation rates will be 25 times slower for oxidation in argon, and 10^7 times slower for oxidation in the CO–CO_2 mixture, compared to oxidation in oxygen. Neither of these oxidation rates will produce measurable oxide layer growth in the time scale of these experiments.

The striking observation of all the oxidation data, ZrO_2-coated and bare substrates alike, is that the oxide layer growth always follows a parabolic dependence upon time. The question which must be answered, given the preceding observations is: what effect can the addition of a ZrO_2 (or $ZrSiO_4$) layer have on the oxidation process without altering the fact that the oxidation process is still diffusion limited even in the presence of the added surface layer? To answer this question, it is instructive to outline the major features of the derivation of a parabolic reaction rate constant for the oxidation of SiC.

The parabolic dependence of the reaction layer thickness, $\Delta\xi$, upon time arises in the following way. The instantaneous rate of growth of the oxide layer is proportional to the flux of oxygen arriving at the SiO_2–SiC interface

$$\frac{d\Delta\xi}{dt} = \tfrac{1}{2} V_m j_O \qquad (2)$$

where V_m is the molar volume of SiO_2, and the 1/2 arises because one mol of oxygen arriving at the SiO_2–SiC interface produces 1/2 mol SiO_2. If it is assumed that the gradient of the chemical potential of oxygen is everywhere constant in the oxide layer then, to a first approximation, the flux of oxygen across the SiO_2 layer, j_O, is given by a modified version of Fick's first law

$$j_O = -\frac{D_O C_O}{RT} \frac{\Delta\mu_O}{\Delta\xi} \qquad (3)$$

where D_O is the diffusion coefficient of oxygen in the oxide layer, C_O is the concentration of oxygen in the oxide layer, $\Delta\mu_O$ is the difference in the chemical potential of oxygen between the surface of the SiO_2 and the SiO_2–SiC interface. The surface of the SiO_2 is either the SiO_2–gas interface, in the case of oxidation of the bare substrates, or the SiO_2–ZrO_2 interface, in the case of oxidation of the composites. Substituting Equation 3 into Equation 2 yields a differential equation describing the oxide layer thickness as a function of time. If we further assumed that both the diffusion coefficient and concentration of oxygen are constant across the oxide layer, then the integral of that differential equation expresses the parabolic dependence of the oxide layer thickness upon time

$$\Delta\xi^2 = 2k_p t \qquad (4)$$

where

$$k_p = \frac{1}{2}\frac{D_O C_O}{RT}\Delta\mu_O \quad (5)$$

Equation 5 shows that the rate of oxidation is controlled by two independent factors: the ability of the oxygen to diffuse through the growing oxide layer (expressed in D_O), and the thermodynamic driving force for the oxidation (expressed by $\Delta\mu_O$).

Putting a layer of ZrO_2 on top of the SiO_2 modifies the oxidation problem in two important ways. An obvious consequence of the presence of this added layer is that to get to the SiC–SiO_2 interface, the oxygen must first cross the ZrO_2 layer, of fixed thickness, and then the growing SiO_2 layer. Either of these two transport steps could limit the rate of reaction. The flux across each layer will be fixed by the difference in chemical potential of oxygen across the layer as well as the thickness of the layer. When the SiO_2 layer is thin, transport across the ZrO_2 layer will limit the rate of reaction because there will be insufficient oxygen supplied at the ZrO_2–SiO_2 interface to satisfy the demand for oxygen at the SiC–SiO_2 interface. If the drop in the oxygen chemical potential across the ZrO_2 layer remains constant with time, the flux of oxygen across that layer will remain constant. Consequently, the thickness of the SiO_2 layer will increase linearly with time. Eventually, however, the SiO_2 layer will grow so thick that transport across it will limit the rate of reaction. At this point, the thickness of the oxide layer will begin to increase with the square root of time. The time at which this crossover from linear to parabolic kinetics occurs will be a function of the diffusion coefficient of oxygen in both the SiO_2 and the ZrO_2 layers, as well as the chemical potential of oxygen at each of the interfaces in the transport path. The conclusion that should be drawn here is that the transport of oxygen across the ZrO_2 layer is not causing the decrease of the oxidation rate of the ZrO_2-coated specimens with respect to the uncoated specimens. If it were, the oxidation kinetics of the coated substrates would be linear in time.

A second effect of the ZrO_2 layer, or any other layer for that matter, is to lower the thermodynamic driving force for oxidation of the SiC. Because oxygen clearly diffuses across the ZrO_2 layer, there must be a drop in the chemical potential of oxygen across the ZrO_2 layer. Because the chemical potential of oxygen at the SiC–SiO_2 interface is determined by the oxidation temperature, the thermodynamic driving force for the oxidation of the SiC, $\Delta\mu_O$, in the composite is less than that for a bare substrate oxidizing under the same external conditions. In other words, compared to the oxidation of the uncoated substrates, the composites are effectively oxidizing under a reduced oxygen partial pressure. The oxidation kinetics for the case of the ZrO_2-coated specimens will remain parabolic, but because the oxidation rate of the SiC is so strongly dependent on the oxygen partial pressure, the oxidation rate will be slower than that for the bare substrates.

4. Conclusions

There are two main conclusions from this work.

1. SiC coated with ZrO_2 oxidizes more slowly than bare SiC, but in both cases the oxidation kinetics are parabolic. One explanation for this phenomenon is that the presence of the ZrO_2 effectively lowers the driving force for the oxidation of the SiC.

2. At oxidation temperatures above 970° C, the ZrO_2 coating reacts with the SiO_2 formed by oxidation to produce $ZrSiO_4$.

Acknowledgement

This work was supported by the N.S.F. under grant no. DMR-8500490.

References

1. W.-K. CHU, J. W. MAYER and M.-A. NICOLET, "Backscattering Spectrometry" (Academic Press, New York, 1978) Chs 1 and 2.
2. L. R. DOOLITTLE, *Nucl. Instrum. Meth.* **B9** (1985) 344.
3. J. A. COSTELLO and R. E. TRESSLER, *J. Amer. Ceram. Soc.* **69** (1986) 674.
4. R. C. A. HARRIS, *ibid.* **58** (1975).
5. W.-J. LU, A. J. STECKL, T. P. CHOW and W. KATZ, *J. Electrochem. Soc.* **131** (1984) 1907.
6. P. J. JORGENSEN, M. E. WADSWORTH and I. B. CUTLER, *J. Amer. Ceram. Soc.* **42** (1959) 613.
7. J. W. HINZE, W. C. TRIPP and H. C. GRAHAM, "The High-Temperature Oxidation of Hot-Pressed Silicon Carbide", in "Mass Transport Phenomena in Ceramics; Materials Science Research", Vol. 9, edited by A. R. Cooper and A. H. Heuer (Plenum Press, New York, 1975) pp. 409–19.
8. P. J. JORGENSEN, M. E. WADSWORTH and I. B. CUTLER, *J. Amer. Ceram. Soc.* **43** (1960) 209.

Received 31 May
and accepted 23 October 1989